Mausam, (1989), **40**, 1, 29-36

551.509.313 (540)

Evaluation of a multi-level primitive equations limited area model for short range prediction over Indian region

U. C. MOHANTY, R. K. PALIWAL*, A. TYAGI* and A. JOHN

Centre for Atmospheric Sciences,
I. I. T., Hauz Khas, New Delhi

(*Received 14 April 1987*)

सार — इस अध्ययन में ऊष्ण कटिबंध में अल्पावधि प्रागुक्ति के लिये फ्लक्स रूप में एक पांच स्तरीय पूर्वग समीकरण सीमित क्षेत्र निदर्श पर विचार किया गया है। इस भौतिक निदर्श में सीमा स्तर, शुष्क संवहनी समायोजन, गहन कपासी संवहन और बड़े पैमाने पर संघनन सम्मिलित हैं। हिमालय सहित पर्वतों का प्रभाव सिग्मा समन्वय संरूपण द्वारा समाविष्ट किया गया है। समय पर निर्भर पार्श्विक सीमा अवस्थाओं के साथ एक दक्ष स्पष्ट विपाटित समय समाकलन योजना का प्रयोग किया गया है। यह अध्ययन दक्षिण-पश्चिम मानसून के दौरान हिन्द महासागर में अल्पावधि सांख्यिकीय मौसम प्रागुक्ति की समस्या से संबंधित है। एफ जी जी ई-1979 की विशेष प्रेक्षित अवधि –II (मॉनेक्स) के दौरान स्थित निम्न विच्छेद, आरम्भिक भ्रमिल, मध्य क्षोभमंडलीय चक्रवात और मानसून अवदाब का प्रतिनिधित्व करने वाले चार विशिष्ट मामलों सहित 48 घंटे तक के निदर्श को समाकलित किया गया है। निदर्श (मॉडल) 48 घंटे के सतही दाब, पवन और तापीय क्षेत्रों के यथोचित अच्छे परिणाम प्रस्तुत करता है। फिर भी, वर्षण पूर्वानुमान बहुत संतोषजनक नहीं पाए गए।

ABSTRACT. A five-level primitive equations limited area model (LAM) in flux form is considered in this study for short range prediction in the tropics. The model physics includes boundary layer, dry convective adjustment, deep cumulus convection and large scale condensation. The effect of mountains including Himalayas is incorporated through sigma coordinate formulation. An efficient split-explicit time integration scheme with time dependent lateral boundary conditions are used. This study addresses the problem of short range numerical weather prediction over Indian sub-continent during SW monsoon season. The model is integrated upto 48 hours with four typical cases representing a cut-off low, onset vortex, mid-tropospheric cyclone and monsoon depression situation during special observing period-II (MONEX) of the FGGE-1979. The model produced reasonably good forecasts of surface pressure, wind and temperature fields up to 48 hours. However, the precipitation forecasts were not very satisfactory.

1. Introduction

It is widely recognised that a high resolution limited area multi-level primitive equations (PE) model is essential to know relatively small scale features over a given region of interest and to predict them for a short range of time. Non-availability of uniformly high quality global analysis and limitations of computer resources encourage research and development of limited area models for numerical weather prediction (NWP). In addition, it is understood that such models developed for short range NWP do not require sophisticated parameterisation schemes to incorporate sub-grid scale processes.

A number of regional multi-level PE models have been developed during the last decade and a detailed review of such models is given by Anthes (1983). However, only a few such models have been developed for tropical region for simulation and prediction of monsoon circulation (Das and Bedi 1978, Krishnamurti *et al.* 1979, Fiorino *et al.* 1982 etc).

In this study, an attempt is made to adapt an idealised time efficient multi-level regional PE model in flux form (developed at Naval Research Laboratory, U.S.A.) for India and its neighbourhood. The performance of this limited area PE model (LAM) for short-range prediction (12-48 hours) of tropical systems (*e.g.*, western disturbances, monsoon depression etc) over India is examined for a number of cases during special observing period (SOP-II) of the FGGE-1979 (MONEX).

2. Description of the model

The horizontal domain of the model is bounded by 30°E-105°E and 7.5°S-45°N with a grid resolution of 2.5° Lat./Long. The model has five sigma ($\sigma = p/p_s$) levels in the vertical, with $\sigma = 0$ as the top and $\sigma = 1$ as the bottom boundary. The orography is derived from U.S. Navy data (obtained from NCAR) and is interpolated to the model grid points (Fig. 1). An overview of the model is given below :

An overview of the model

Domain	: 31×22 (7.5°S-45°N, 30°E-105°E) : Flexible
Independent variables	: λ, ϕ, σ, t
Prognostic variables	: u, v, T, q, p_s
Diagnostic variables	: ϕ, $\dot{\sigma}$

*Directorate of Meteorology, Indian Air Force, Air HQ (VB), New Delhi

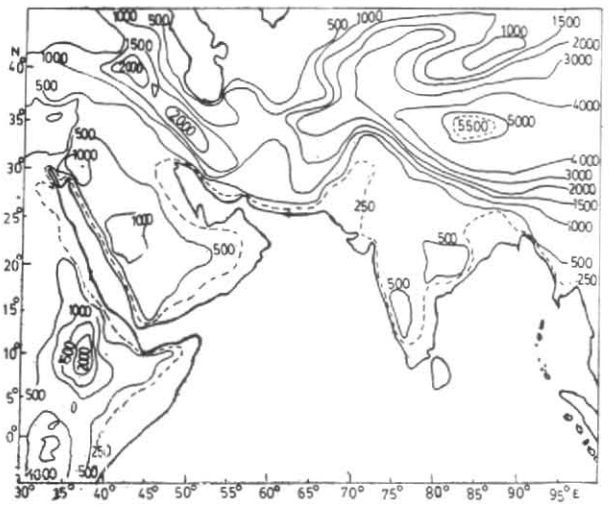

Fig. 1. Model orography (m)

Vertical levels	: Five, $\sigma = .1, .3, .5, .7, .9$ (Flexible)
Grid system	: Arakawa C-grid
Space finite difference scheme	: Second order accuracy
Time integration scheme	: Split-explicit time integration scheme
Time step	: $\triangle t = 1200$ sec (20 minutes)
$\triangle\lambda$, $\triangle\phi$	: 2.5 Lat./Long. (Flexible)
Horizontal diffusion	: Linear fourth order
Initialisation	: Dynamic initialisation Okamura scheme (Nitta 1969)
Physical processes	: Dry convective adjustment, deep cumulus convection (Kuo scheme) (Anthes 1977) with convective precipitation Large scale stratified precipitation with RH $\geqslant 95\%$ Planetary Boundary Layer— Monin-Obukhov Similarity Theory Air-sea sensible heat exchange and evaporation from ocean
Computer time for 24-hr forecast	: 990 sec CPU Time on Cyber 170/730 system.

2.1. *Model equations*

The primitive equations governing the motion of the atmosphere, appropriate to a meso-scale quasi-hydrostatic, baroclinic system are represented in flux form in spherical coordinates. The model with five prognostic and two diagnostic equations (*viz.*, the zonal and meridional momentum, the thermodynamic, the moisture continuity, the surface pressure tendency, the hydrostatic and the continuity equations) for the seven meteorological variables (u, v, T, q, p_s, ϕ and n) forms a closed system as given below :

$$\frac{\partial}{\partial t}(p_s u) + \frac{1}{h_x h_y}\left[\frac{\partial}{\partial x}(p_s u h_y u) + \frac{\partial}{\partial y}(p_s v h_x u) + \right.$$
$$\left. + \frac{\partial}{\partial \sigma}(p_s n u) - f p_s v + \frac{p_s u v}{h_x h_y}\frac{\partial}{\partial y}h_x \right] = -\frac{p_s}{h_x}\frac{\partial \phi}{\partial x} -$$
$$- \frac{RT}{h_x}\frac{\partial p_s}{\partial x} + p_s F_u \qquad (1)$$

$$\frac{\partial}{\partial t}(p_s v) + \frac{1}{h_x h_y}\left[\frac{\partial}{\partial x}(p_s u h_y v) + \frac{\partial}{\partial y}(p_s v h_x v)\right] +$$
$$+ \frac{\partial}{\partial \sigma}(p_s n v) + f p_s u - \frac{p_s u^2}{h_x h_y}\frac{\partial}{\partial y}h_x = -\frac{p_s}{h_y}\frac{\partial \phi}{\partial y} -$$
$$- \frac{RT}{h_y}\frac{\partial p_s}{\partial y} + p_s F_v \qquad (2)$$

$$\frac{\partial}{\partial t}(p_s T) + \frac{1}{h_x h_y}\left[\frac{\partial}{\partial x}(p_s u h_y T) + \frac{\partial}{\partial y}(p_s v h_x T)\right] +$$
$$+ \left(\frac{\sigma}{\sigma_0}\right)^{\kappa}\frac{\partial}{\partial \sigma}(p_s n \theta) + \frac{RT}{c_p}\widetilde{D} -$$
$$- \frac{RT}{c_p}\left(\frac{u}{h_x}\frac{\partial p_s}{\partial x} + \frac{v}{h_y}\frac{\partial p_s}{\partial y}\right) = p_s H_T + p_s F_T \qquad (3)$$

$$\frac{\partial}{\partial t}(p_s q) + \frac{1}{h_x h_y}\left[\frac{\partial}{\partial x}(p_s u h_y q) + \frac{\partial}{\partial y}(p_s v h_x q)\right] +$$
$$+ \frac{\partial}{\partial \sigma}(p_s n q) = p_s H_q + p_s F_q \qquad (4)$$

$$\frac{\partial p_s}{\partial t} = -\widetilde{D} \qquad (5)$$

$$\frac{\partial \phi}{\partial \sigma} = -\frac{RT}{\sigma} \qquad (6)$$

$$\frac{\partial (p_s n)}{\partial \sigma} = \widetilde{D} - D \qquad (7)$$

Here p_s is the surface pressure, u and v the zonal and meridional wind components respectively, f the coriolis parameter, ϕ the geopotential, T the temperature, q the specific humidity, $n = d\sigma/dt$ the vertical velocity in sigma coordinate, R the gas constant for dry air, θ the potential temperature, c_p the specific heat capacity of dry air at constant pressure, D the divergence and $\widetilde{D}$ the vertically integrated horizontal and mass divergence. The vertical friction terms which include surface fluxes and vertical and horizontal diffusion of momentum, heat and moisture are represented by F_u, F_v, F_T, and F_q respectively. Further, the heat and moisture source/sink terms are represented by H_T and H_q respectively. h_x and h_y represent the map factors.

2.2. *Finite difference form of the model equations*

The space derivative terms in the model equations are approximated by a second order accurate, quadratic conserving finite difference scheme over a staggered horizontal Arakawa C-grid (Arakawa and Lamb 1977).

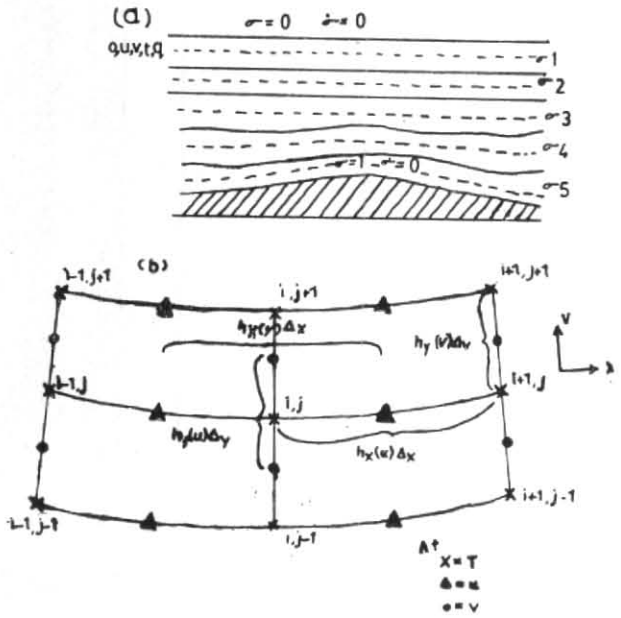

Fig. 2. (a) Vertical σ levels and (b) Arakawa C-grid

This scheme is found to be suitable to suppress two-grid length computational gravity wave noise and to conserve the integral properties. T, ϕ, q and n are computed at the mass points (i, j) while u is computed at the mid-points of mass points along x-axis and v at mid-points along y-axis (Fig. 2). Any parameter $A^K_{i,j}$ which represents the value of A at (i, j)th horizontal grid point on Kth level, is approximated in this scheme as :

$$\frac{\delta}{\delta_x} A^K_{ij} = \delta_x A^K_{ij} = \left(A^K_{i+\frac{1}{2}, j} - A^K_{i-\frac{1}{2}, j} \right) \Big/ h_{ij}(x)\, \triangle x_{ij}$$

and $$< A^K_{ij} >_x = \left(A^K_{i+\frac{1}{2}, j} + A^K_{i-\frac{1}{2}, j} \right) \Big/ 2$$

where δ_x represents finite difference, $< >_x$ an average along x-direction,

$$\triangle x_{ij} = (x_{i+1/2,\, j} - x_{i-\frac{1}{2},\, j})$$

and $h_{ij}(x)$ is map factor in x direction at (i, j)th grid point for A. The vertical differentiation and averaging are also carried out in a similar manner. The finite difference form of the u-momentum Eqn. (1) is as given below :

$$\frac{\partial}{\partial t} < (p_s)_{i,j} >_x u^K_{i,j} + < (p_s)_{i,j} >_x \delta_x \phi_{ij}{}^K +$$

$$+ < RT_{ij}{}^K >_x \delta_x (p_s)_{ij} = A_{ij}{}^K \qquad (8)$$

where,

$$A_{ij}{}^K = - \frac{1}{< h_{ij}(y) >_x} \delta_x \left[\ll h_{ij}(y)\, (p_s)_{ij} >_x u_{ij}{}^K >_x \cdot \right.$$

$$\left. < u_{ij}{}^K >_x \right] - \frac{1}{< h_{ij}(x) >_x} \delta_y \left[\ll h_{ij}(x)\, (p_s)_{ij} >_y v_{ij}{}^K >_x \cdot \right.$$

$$\left. < u_{ij}{}^K >_y \right] - \left[< (p_s)_{ij}\ n^{K+1/2} >_x < u_{ij}{}^K >_\sigma - \right.$$

$$\left. - < (p_s)_{ij}\ n_{ij}{}^{K-1/2} >_x < u_{ij}{}^{K-1} >_\sigma \right] \Big/ \triangle \sigma^K +$$

$$+ \ll f_j (p_s)_{ij} >_y v_{ij}{}^K >_{x,y} - < (p_s)_{ij} >_x u_{ij}{}^K < v_{ij} >_{x,y}$$

$$\times \frac{\delta_x h_{ij}(x)}{< h_{ij}(x) >_x < h_{ij}(y) >_y} + < (p_s)_{ij} >_x F_{ij}{}^K (u)$$

Similarly model Eqns. (2)-(7) are transformed into appropriate finite difference form. Separating the temperature into a mean part, T^*, which varies only in the vertical and a deviation part, T' ($\equiv T - T^*$), the model Eqns. (1)-(7) are transformed into matrix form for programming and computational purposes.

2.3. *Time integration scheme*

The model uses an efficient split-explicit time integration scheme, which is found to be computationally economical than an explicit scheme (Madala 1981). In this scheme, the terms in the prognostic Eqns. (1)-(5) are split according to the vertical modes into those governing the Rossby and the gravity modes. The model is integrated for the individual modes using different time steps as required by the respective CFL criteria. This is unlike the technique of Gadd (1978) wherein only two time steps are used, one commonly for all the gravity modes and the other for the Rossby modes. The implementation of varying time steps is the basis of split-explicit time integration scheme used in the present work. For the detail description of this method, its properties and application, it is suggested to refer Madala (1981) and Mohanty *et al.* (1987).

2.4. *Boundary conditions*

A time dependent lateral boundary scheme of Perkey and Kreitzberg (1976) is incorporated in the model. This scheme provides a 'porous-sponge' in the boundary zone. It makes use of the model calculated tendencies for extrapolation of the boundary values of the variables. The prediction of any dependent variable 'M' is given by :

$$M_n(I) = M_p(I) + W(I) \left. \frac{\partial M_m}{\partial t} \right|_I \triangle t \qquad (9)$$

where the subscript n and p denote the new value after the boundary condition and the previous value at the preceding time step respectively. The model calculated tendency of the variable is denoted by 'm'. $W(I)$ is the weightage factor whose values are assigned as 0.4, 0.7 and 0.9 for the boundary grid points, one grid point interior and two grid points interior from the boundary respectively. The model tendency at the boundary points are obtained by linear extrapolation of the model calculated tendencies at the two interior grid points.

2.5. *Horizontal diffusion*

In order to take into account the effect of energy associated with unresolved sub-grid scale processes, a horizontal diffusion scheme is used in the numerical models. In the case of limited area models, such a horizontal smoothing substantially controls the computational noise generated on the artificial lateral boundaries. In this study, a simple linear fourth order diffusion is applied on sigma coordinate surfaces for the zonal and meridional wind components :

$$F_{HX} = K_H \nabla^2 (\nabla^2 X) \qquad (10)$$

where $X = u$ or v and K_H is the horizontal eddy viscosity,

2.6. *Physical processes*

Various physical processes such as boundary layer, stratified precipitation, dry and moist convection etc relevant to short range weather prediction are parameterised in the model. However, short and long wave radiations which are assumed to be less important for a short range forecast (up to 48 hours), are not included.

The planetary boundary layer is parameterised in the model to include the effects of friction, air-sea sensible heat exchange and diffusion of heat, moisture and momentum. The vertical exchange of heat, moisture and momentum are parameterised in a similar way as described by Manabe *et al.* (1965). The surface friction is considered through the drag law with a drag coefficient C_D (2.5×10^{-3} for land and 1.0×10^{-3} over water). Bulk aerodynamic formulae are used to include the latent and sensible heat exchanges with the exchange coefficient value of C_E as 1.0×10^{-3} over water and 0.0 over land.

The treatment of deep cumulus convection in the model is based on Kuo (1965, 1974) as subsequently modified by Anthes (1977) where in the available moisture is partitioned into two parts, *viz.*, a part which is used for the moistening of the environment and the second part for heating. Large scale condensation over regions of ascent of stable saturated air is computed by limiting the humidity values to their saturation values (95% of RH). If any level is super-saturated, the excess moisture is allowed to condense out and fall to the next lower level and evaporate or continue to fall depending upon the state of saturation at that level.

A dry convective adjustment scheme as proposed by Manabe *et al.* (1965, 1970) is incorporated in the model. This scheme removes the absolute instability, if it has occurred at any grid point, by neutralizing the lapse rate while conserving the dry static energy in the entire column. The instability is explicitly removed *via* an equal energy adjustment after every two hours of integration of the model.

3. Data and initialisation

GARP summer monsoon experiment (SOP-II) during FGGE year (1979) provided an excellent data base for NWP studies. For the first time, a truly tropical belt data set has been obtained over the data-sparse region through various conventional and non-conventional means and for a complete set of atmospheric data over monsoon region ever obtained. The final form of the gridded data set called as FGGE level III-b analysis, produced at the European Centre for Medium Range Weather Forecasts, U.K. is used for this study.

Four typical situations, which represent different facets of the SW monsoon during 1979, are selected in this study to evaluate the performance of the limited area model for short range prediction up to 48 hours. These are :

(*a*) A case of a cut-off low over northwest India and neighbourhood during pre-monsoon (22 May 1979).

(*b*) Case of monsoon onset vortex over Arabian Sea (14 June 1979).

TABLE 1

Time series of mean kinetic energy and mean total energy during one day forecast

Time (hr)	$\|KE\|$ ($\times 10^2 m^2/sec^2$)	$\|TE\|$ ($\times 10^5 m^2/sec^2$)
0	3.4537	1.3238
3	3.4548	1.3227
6	3.4552	1.3221
9	3.4571	1.3217
12	3.4586	1.3212
15	3.4594	1.3208
18	3.4613	1.3197
21	3.4624	1.3195
24	3.4629	1.3186

(*c*) Case of a mid-tropospheric cyclone off Gujarat coast (26 June 1979).

(*d*) Case of a monsoon depression (5 July 1979).

In all the cases, 12 GMT data of 11 standard pressure levels (1000, 850, 700, 500, 400, 300, 200, 100, 70, 50 and 30 mb) at regular grid points of 1.875° Lat./Long. has been interpolated to the model grid points at five sigma levels (as discussed in section 2).

An effective dynamic initialisation scheme of Okamura (Nitta 1969) is used to an adiabatic version of the model to achieve a balance between mass and velocity fields before forward time integration of the model. Details about the performance of this initialisation scheme with 12 GMT of 22 May 1979 data-set is described by Mohanty *et al.* (1987) and hence will not be repeated here.

4. Results and discussion

The performance of the model in simulation and prediction (up to 48 hours) with the input of the four typical cases, as mentioned in section 3, is critically examined. The results are presented in the following three sub-sections.

4.1. *Model characteristics*

Before evaluating the forecast performance of the model, it is necessary to examine the conserving properties and behavioral characteristics of the limited area model during its forward integration, as a number of approximations (*e.g.*, lateral boundaries, finite difference scheme, time integration etc) are involved in the formulation of the model. In this sub-section, some such parameters as the level mean kinetic energy, mean total energy, mean divergence, mean absolute tendencies of u, v, T and also surface pressure and n (vertical velocity in sigma coordinate) at a given location (15°N, 60°E), are monitored at each of the time step during the entire length of integration of the model (48 hours). However, results of the first 24 hours of integration are presented as no significant change in the trend of these parameters are observed beyond this period.

TABLE 2

Root mean square error of 24 hours and 48 hours forecast
(u, v and V in m/sec, T in °C and p_s in mb)

Levels/Variables		Forecast period: 24 hours 1	2	3	4	Mean	Mean V	48 hours 1	2	3	4	Mean	Mean V
300 mb	u	3.8	4.1	3.6	3.6	3.8		5.5	4.9	6.1	6.8	5.8	
	v	4.4	4.2	4.0	3.7	3.8	5.6	7.0	7.5	6.6	5.1	6.5	8.7
	T	2.4	2.3	2.0	1.9	2.2		3.1	2.9	2.8	2.6	2.8	
500 mb	u	2.1	2.7	2.8	3.8	2.8		7.0	6.9	6.2	5.1	6.3	
	v	2.8	1.9	2.0	2.1	2.2	3.6	2.3	3.1	2.4	2.7	2.6	6.8
	T	1.0	1.4	1.3	1.2	1.2		1.4	1.4	1.6	2.1	1.6	
700 mb	u	3.2	2.9	2.7	2.6	2.8		4.4	3.9	4.6	5.0	4.5	
	v	2.2	1.7	2.6	2.1	2.1	3.5	3.2	3.9	3.4	3.8	3.3	5.6
	T	0.9	1.1	1.2	0.9	1.0		1.1	1.5	1.8	2.1	1.6	
850 mb	u	2.9	2.7	2.6	3.0	2.8		3.1	3.1	3.2	3.9	3.3	
	v	2.2	1.9	2.0	2.2	2.1	3.5	2.7	2.4	2.7	3.1	2.7	4.3
	T	1.6	1.5	1.3	1.1	1.4		1.4	1.3	1.5	1.9	1.5	
	p_s	1.7	1.6	1.9	2.0	1.8		1.8	2.1	2.3	2.0	2.1	

Case 1—22 May 1979 : 1200 GMT (cut-off low)
Case 2—14 June 1979 : 1200 GMT (onset vortex)
Case 3—26 June 1979 : 1200 GMT (mid-tropospheric cyclone)
Case 4—5 July 1979 : 1200 GMT (monsoon depression)

Table 1 depicts the change in the mean kinetic energy (KE) and total energy (TE) during the first 24 hours of integration of the model. It is seen from this figure that during this period the mean KE and TE remain almost constant ($< 10\%$ change). Similarly, the model is also found to conserve the total mass over the domain. Thus, the model satisfies an important property to conserve mass and energy to a desired level during its integration up to 48 hours.

4.2. *Evaluation of the forecast performance*

In order to evaluate the efficiency of the model in the prediction of meteorological variables (up to a period of 48 hours), the forecast results are compared with the corresponding observed field in respect of the four synoptic cases under study. Both qualitative and quantitative comparisons are carried out. For this purpose, the root mean square (r.m.s.) error of the forecast fields of u, v, T and p_s at 24 and 48 hours from the respective verification fields are presented in Table 2. The r.m.s. errors are estimated over an interior domain (2.5°N-30°N, 45°E-92.5°E) in order to avoid the region close to the lateral boundaries. In general, it is seen from the Table 2 that the models performed well for all the four cases. The r.m.s. error of u, v, T and r.m.s. vector wind error at all the levels are found to be reasonably small and comparable to similar results presented for tropics (Heckley 1985). The r.m.s. error of surface pressure is about 2 mb during 48 hours forecast.

The r.m.s. error of zonal wind is found to be higher than that of the meridional wind except in the upper troposphere (300 mb). In general, the r.m.s. vector wind error is found to increase with height. The mean r.m.s. vector error of wind at 850 mb is 3.5 m/sec and 4.3 m/sec vector wind at 24 and 48 hours respectively. This result is found to be comparatively lesser than the r.m.s. error of vector wind obtained from a number of global models for the tropical belt (30°S-30°N) at 850 mb for 11 June 1979 (Temperton *et al.* 1983). However, such a comparison may not be considered optimistic in view of the small and different samples of data used for these studies. The r.m.s. error of temperature is found to be small and it even does not exceed 2°C after 48 hours of forecast.

4.3. *Prediction of monsoon depression over the Bay of Bengal*

Though a detailed qualitative analysis and comparison of the forecasts and respective observed fields are carried out for all the four synoptic cases mentioned in section 3, in this sub-section we have restricted the presentation to the case of monsoon depression (5-7 July 1979).

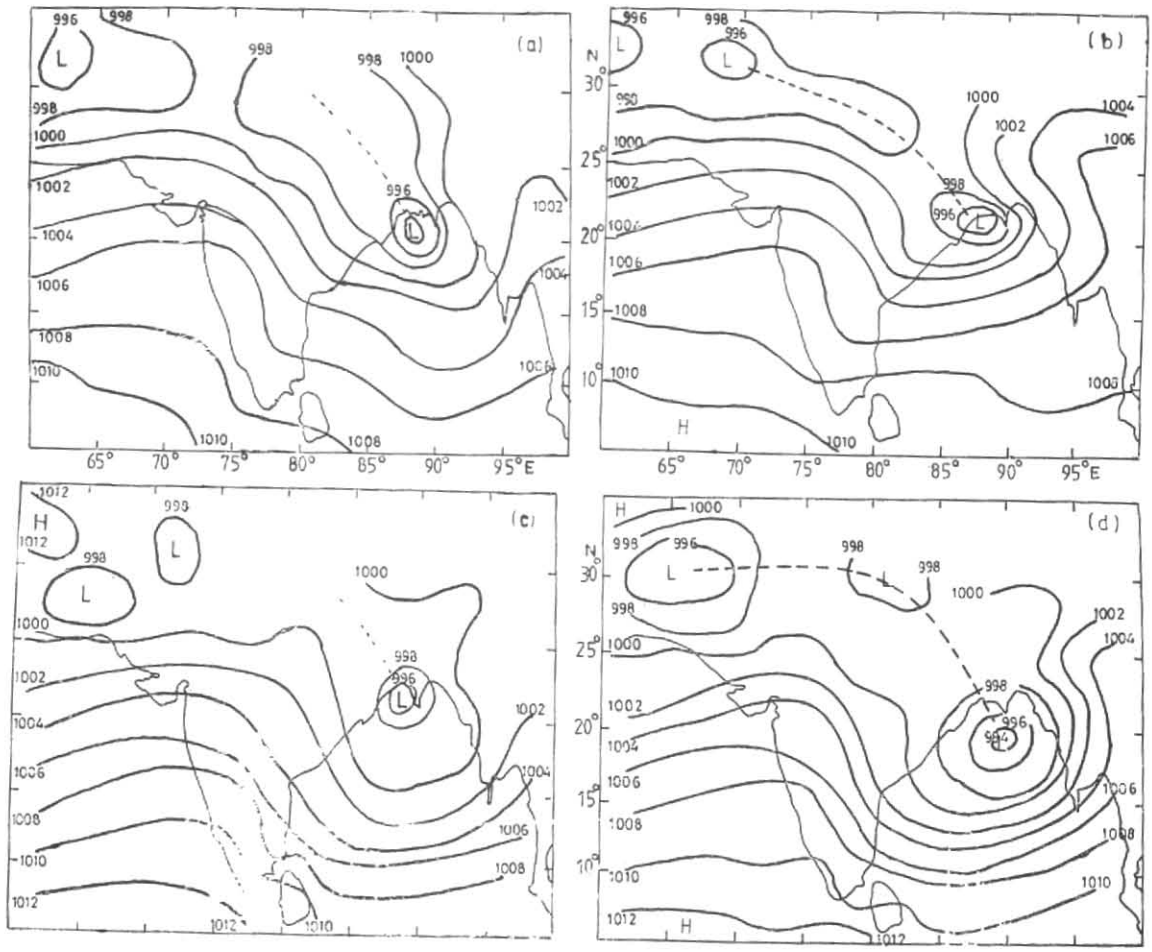

Fig. 3. Mean sea level pressure analysis of (a) 24 hours forecast for 05 July 1979 (12 GMT), (b) 48 hours forecast for 05 July 1979 (12 GMT) and (c)-(d) corresponding verification analyses

Surface pressure, wind, temperature and rainfall analysis of forecasts and the corresponding observed fields are presented in this sub-section.

4.3.1. *Surface pressure distribution*

Figs. 3 (a-d) depict 24 and 48 hr forecast of surface pressure isobaric distribution and corresponding observed analyses (12 GMT, 6-7 July 1979). On 5 July 1979 at 12 GMT, a low pressure area was centred close to 21°N and 91°E (initial field for the model). It intensified into a depression on 6 July (centred at 20°N, 90° E) and subsequently into a deep depression at 12 GMT of 7 July centred close to 20°N, 88°E. The 24 hours forecast clearly brings out the intensification of the initial low into a depression almost at the same position as the observed analysis. However, further intensification into a deep depression has not been reflected in the 48 hours forecast. Moreover, the predicted location of the depression in the 48 hours forecast is about two degrees to the north as compared to the actual position. However, the semi-permanent features like the monsoon trough and heat low over NW India and Pakistan are reasonably well simulated up to 48 hours by the model.

4.3.2. *Streamline-isotach analysis*

Figs. 4 (a-d) present the streamline isotach pattern of 24 and 48 hours forecasts and the corresponding analysis at 700 mb. The cyclonic circulation associated with the monsoon depression is well predicted in the 24 and 48 hours model forecasts. The location of the centre of the circulation in the 24 hours forecast is almost same as in the actual analysis. However, the 48 hours forecast position of the centre, like in the case of surface pressure, is about two degrees to the north as compared to the observed location. Moreover, the intensification of the circulation as evident from the easterly maxima (10 m/sec) to the north of the system, is not reflected in the 48 hours forecast. The broad belt of strong westerlies over Arabian Sea, Peninsular India and Bay of Bengal is well simulated by the LAM. However, the model produced a strong anticyclonic eddy between 50° and 70°E, between equator and 5°N, in the 48 hours forecast which is not observed in the corresponding verification field. This is probably due to the lateral boundary conditions for the LAM.

4.3.3. *Rainfall distribution*

Fig. 5(a) depicts the observed 24 hours precipitation from raingauge and satellite data calibration from

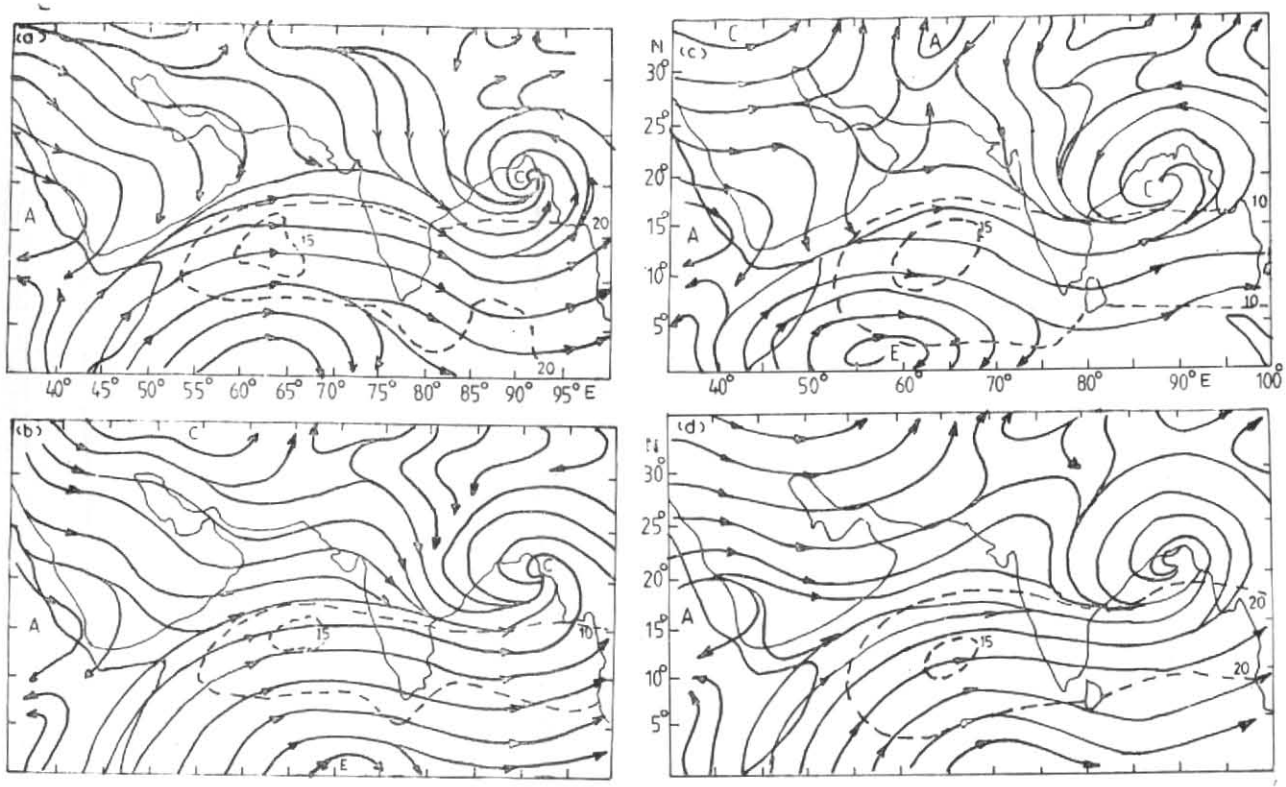

Fig. 4. Same as Fig. 5 but for streamline isotach analysis (m/s) of wind field at $\sigma = 5.7$ (approx. 700 mb)

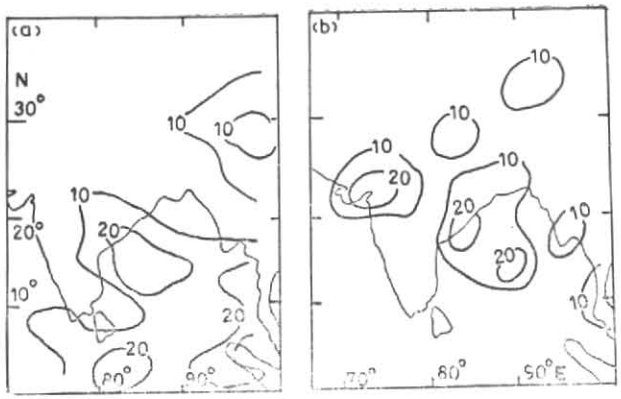

Fig. 5. Precipitation (mm) for 24 hours ending 07 July 1979 (00 GMT) : (a) observed & (b) forecast

6 July to 7 July 1979, 00 GMT (Krishnamurti 1983). The 24 hours predicted distribution of precipitation for the same period is shown in Fig. 5(b). It is seen from Fig. 5 that the model predicted precipitation rate in the WSW sector of the monsoon depression is almost similar to the observed rate of precipitation. However, the model has either failed to simulate or has underestimated precipitation rate over SE Asia, Eastern Himalayas, Kerala coast, Sri Lanka and adjoining oceanic areas. Also the model forecast shows a spurious region of rainfall over Gujarat and adjoining areas.

5. Conclusions

Performance of a five-level primitive equations limited area model in flux form has been evaluated with four typical cases to predict different aspects of monsoon over Indian region using FGGE level-IIIb data sets. The forecast verifications show a considerable skill in predicting surface pressure, wind and temperature fields up to a period of 48 hours. The forecast error of surface pressure in 48 hours does not exceed 2 mb and mean forecast temperature error lies within 1°-2°C. The mean forecast error of vector wind increases with height in the troposphere and the maximum value does not exceed 6 and 9 m/sec in 24 and 48 hours respectively at 300 mb. The monsoon trough and other semi-permanent features of SW monsoon are well simulated by the model. The movement of monsoon depression is reasonably well predicted up to 48 hours. However, though the location of the heavy precipitation in the field of monsoon depression is well brought out, considerable discrepancy in the amount of precipitation is observed.

Though, the inter-comparison of the forecast error statistics of this model with similar models in tropics is very encouraging, due to the limited number of cases examined in this study, the conclusions may not be considered either general or comprehensive. The forecast errors suggest improved vertical resolution, particularly in the boundary layer, inclusion of shallow convection and radiation and suitable modifications in the existing planetary boundary layer and deep cumulus convection schemes in the model to remove the conceptual deficiencies.

Acknowledgement

The authors express their gratitude to Dr. R.V. Madala of Naval Research Laboratory, U.S.A. for providing an idealised version of the code and for many valuable discussions during its implementation at I.I.T., New Delhi. We are grateful to Prof. P.K. Das for many useful discussions, encouragement and a careful review of the manuscript. We are also thankful to Air Vice Marshal R. K. Mathur, Prof. M. P. Singh and Dr. S. Sethuraman (N.C.S.U.), S.C. Madan, K. J. Ramesh and V.B. Sarin have provided useful computational help. This work was partly supported by Aeronautics Research and Development Board of Ministry of Defence and C.S.I.R.

References

Anthes, R.A., 1977, A cumulus parameterisation scheme utilizing a one dimensional cloud model, *Mon. Weath. Rev.*, **105**, 270-286.

Anthes, R.A., 1983, Regional Models of the Atmosphere in Middle Latitudes, *Mon. Weath. Rev.*, **111**, 1306-1335.

Das, P.K. and Bedi, H.S., 1978, The inclusion of Himalayas in a primitive equation model, *Mausam*, **29**, pp. 375-383.

Fiorino, M., Harrison, E.J. and Marks, D.G., 1982, A comparison of the performance of two operational dynamic tropical forecast models, *Mon. Weath. Rev.*, **110**, 651-656.

Gadd, A.J., 1978, A split-explicit integration scheme for numerical weather prediction, *Quart. J. R. met. Soc.*, **104**, 569-582.

Heckley, W.A., 1985, The performance and systematic errors of the ECMWF forecasts 1982-1984, ECMWF Tech. Rep. No. 53.

Krishnamurti, T.N, Pan, H., Chang, C.B., Ploshay, J. and Oodally, W., 1979, Numerical Weather Prediction for GATE., *Quart. J. R. met. Soc.*, **105**, 979-1010.

Krishnamurti, T.N., Cocke, S., Pasch R. and Low-Nam, S., 1983, Precipitation estimates for raingauge and satellite observations. Florida State University Report No. 83-7, Dept. of Meteorology, FSU Tellahassee, Florida, 1-376.

Kuo, H.L., 1965, On formation and intensification of tropical cyclones through latent heat release by cumulus convection, *J. atmos. Sci.*, **22**, 40-63.

Kuo, H.L., 1974, Further studies of the parameterisation of the influence of cumulus convection on large scale flow, *J. atmos. Sci.*, **31**, 1232-1240.

Madala, R., 1981, *Finite difference techniques for vectorized fluid dynamic calculations*, Springer-Verlag, 56-70.

Mohanty, U.C., Paliwal, R.K., Tyagi, A. and Sarin, V.B., 1987, A suitable scheme of dynamic initialization for a multi-level primitive equations model in tropics (Communicated to *Mausam*)

Manabe, S., Smagominsky, I. and Strickler, R.F., 1965, Simulated climatology of a general circulation model with hydrologic cycle, *Mon. Weath. Rev.*, **93**, 769-798.

Manabe, S., Holloway, J.L. and Stone, H.M., 1970, Tropical circulation in a time-integration of a global model of the atmosphere, *J. atmos. Sci.*, **27**, 580-613.

Nitta, T., 1969, Initialisation and analysis for the PE model, Proc. WMO/IUGG, Symp. on NWP, Tokyo.

Perkey, D.J. and Krietzberg, C.W., 1976, A time dependent lateral boundary scheme for limited area primitive equation models, *Mon. Weath. Rev.*, **104**, 744-755.

Temperton, C., Krishnamurti, T.N., Pasch, R. and Kitade, T., 1983, WGNE Forecast comparison experiments Report No. 6 (pp. 1-104), WCRP, published by W.M.O., Geneva, Switzerland.